Assembly of Aqueous-Cored Calcium Phosphate Nanoparticles for Drug Delivery

Hartley T. Schmidt, Ben L. Gray, Philip A. Wingert, and Agnes E. Ostafin*

Department of Chemical and Biomolecular Engineering, and Center for Molecularly Engineered Materials, University of Notre Dame, Notre Dame, Indiana 46556

Received April 13, 2004. Revised Manuscript Received July 12, 2004

A synthesis strategy for aqueous-cored calcium phosphate nanoparticles is presented that combines ease of preparation, reproducibility, size control, stability, and mean thickness control. Suspension stability and shell thickness control were achieved through the introduction of a "capping" molecule, carboxyethylphosphoric acid (CEPA). Using this method, suspensions of calcium phosphate shells were produced with a size distribution of 120−185 ± 50 nm and predictable mean shell thickness from 10 to 40 nm that were stable up to a month, even in the presence of 200 mM salt and 2.5 g/dL albumin.

Introduction

The synthesis of biocompatible and biodegradable nanoparticles for applications as diagnostic markers or drug delivery in vivo is a vigorous area of current research.[1−8] To be successful, the particles need to be small enough to travel unimpeded through the vasculature, versatile enough to carry a wide variety of agents, able to survive for an extended period of time, and simple to manufacture. Liquid-filled liposomes stabilized by silica,[9,10] calcium phosphate,[11] or polymers[12−15] are promising materials. The reinforcing coating temporarily protects the inherently fragile liposome and its contents while in the bloodstream, and provides a platform on which to construct a surface capable of chemical recognition and the ability to elude the reticuloendothelial system.

Calcium phosphate coated liposomes may have a unique usefulness for the delivery of bone and dental therapeutics.[16,17] Calcium phosphate is biocompatible[18] and biodegradable,[19,20] and is native to the body as the principle mineral component of teeth and bones.

The reaction chemistry of calcium phosphate is complex and presents challenges for synthesis, scale-up, and manufacture. Our previous work[11] demonstrated that it was possible to deposit nanometers-thick coatings on nanosized liposomes. In this work, we present a more detailed understanding of the reaction chemistry. Using a simplified batch reaction strategy it was possible to obtain improvement in the long-term stability of particle suspensions as well as control of particle size and coating thickness.

Materials and Methods

Materials. 1,2-Dioleoyl-*sn*-glycero-3-phosphate (DOPA) lipid (MW 722.96 g/mol, T_c−8 °C, and saturation 18:1) was obtained as a lyophilized powder in sealed 25-mg vials and stored at −80 °C (Avanti Polar Lipids). Carboxyethylphosphoric acid (CEPA) (Sigma-Aldrich), $CaCl_2$, H_3PO_4, NaCl, NaOH, acetone, glacial acetic acid, and lyophilized bovine serum albumin (BSA) (Fisher) were used without further purification. Snakeskin dialysis tubing with a MWCO of 3500 Da was obtained from Pierce. Cellulose acetate (CA) syringe filters with 0.45-μm pore size were obtained from Millipore. A handheld extrusion apparatus with 100-nm polycarbonate (PC) filters (Millipore) was obtained from Avanti. Deionized (DI) water used for experiments had a resistivity greater than 18 MΩ.

Preparation of Calcium Phosphate Nanoparticles. Syntheses were performed in 50-mL glass beakers cleaned by scrubbing with a small amount of glacial acetic acid, rinsing with hot tap water 5×, rinsing with DI water 2×, rinsing with acetone, rinsing with hot tap water 5×, rinsing with DI water 5×, and dried in an oven at 200 °F for 2 h. Liposomes were prepared by extrusion of 1 mL of 0.693 mM DOPA lipid in DI water solution through a 100-nm PC filter at room tempera-

* Corresponding author. E-mail: aostafin@nd.edu.

(1) Hans, M. L.; Lowman, A. M. *Curr. Opin. Solid State Mater. Sci.* **2002**, *4*, 319.
(2) Cui, Z. R.; Mumper, R. J. *Crit. Rev. Ther. Drug* **2003**, *2−3*, 103.
(3) Anderson, J. M.; Shive, M. S. *Adv. Drug Delivery Rev.* **1997**, *1*, 5.
(4) Bagwe, R. P.; Zhao, X.; Tan. We. *Biomaterials* **2004**, *25*, 723.
(5) Chen, J.-F.; Ding, H.-M.; Wang. J.-X.; Shao, L. *Biomaterials* **2004**, *4*, 723.
(6) Kossovsky, N.; Gelman, A.; Sponsler, E. E.; Hnatyszyn, H. J.; Rajguru, S.; Torres, M.; Pham, M.; Crowder, J.; Zemanovich, J. *Biomaterials* **1994**, *15*, 1201.
(7) Panyam, J.; Labhasetwar, V. *Adv. Drug Delivery Rev.* **2003**, *3*, 329.
(8) Zimmer, A.; Kreuter, J. *Adv. Drug Delivery Rev.* **1995**, *1*, 61.
(9) Hubert, D. H. W.; Jung, M.; Frederik, P. M.; Bomans, P. H. H.; Meuldijk, J.; German, A. L. *Adv. Mater.* **2000**, *17*, 1286.
(10) Hentze, H.-P.; Raghavan, S. R.; McKelvey, C. A.; Kaler, E. W. *Langmuir* **2003**, *19* (4), 1069.
(11) Schmidt, T.; Ostafin, A. *Adv. Mater.* **2002**, *7*, 532.
(12) Hotz, J.; Meier, W. *Langmuir* **1998**, *5*, 1031.
(13) Sehgal, S.; Rogers, J. A. *J. Microencapsulation* **1995**, *1*, 37.
(14) Kawakami, K.; Nishihara, Y.; Hirano, K. *J. Phys. Chem. B.* **2001**, *105* (12), 2374.
(15) Heldt, N.; Gauger, M.; Zhao, J.; Slack, G.; Pietryka, John,; Li, Y. *React. Funct. Polym.* **2001**, *1−3*, 181.
(16) Sun, J.-S.; Tsuang, Y.-H.; Liao, C.-J.; Liu, H.-C.; Hang, Y.-S.; Lin, F.-H. *J. Biomed. Mater. Res.* **1997**, *3*, 324.
(17) Lucas, L. C.; Lacefield, W. R.; Ong, J. L.; Whitehead, R. Y. *Colloids Surf., A* **1993**, *2*, 141.
(18) Habibovic, P.; Barrere, F.; Van Blitterswijk, C. A.; De Groot, K.; Layrolle, P. *J. Am. Chem. Soc.* **2002**, *3*, 517.
(19) Lu, J. X.; Descamps, M.; Dejou, J.; Koubi, G.; Hardouin, P.; Lemaitre, J.; Proust, J.-P. *J. Biomed. Mater. Res.* **2002**, *4*, 408.
(20) Chu, T. C.; He, Q.; Potter, D. E. *Journal of Ocular Pharmacology and Therapeutics* **2002**, *18*, 507.

10.1021/cm040056i CCC: $27.50
Published on Web 10/29/2004

ture 11× until the mean size distribution as measured by dynamic light scattering (DLS) was comparable to the pore size of the filter. After extrusion, the liposomes were allowed to rest for at least 1 h and were used within 48 h after extrusion. Dynamic light scattering (DLS) measurements revealed no noticeable affect on suspension quality during this period.

To coat the liposomes with calcium phosphate, 50 mL of DI water was mixed with 10 μL of 1 M phosphoric acid and 40 μL of 1 M NaOH (pH ~10). A 100 μL portion of 0.1 M $CaCl_2$ and 150 μL of liposomes prepared as described were added to this solution within 5 s of each other using a volumetric pipet while the suspension was stirred magnetically at 400 rpm at room temperature (typically 25° C). At selected times thereafter (10, 30, 60, 90, 120, 150, and 180 min), 50 μL of 0.1 M CEPA was pipetted into the stirring solution to halt the reaction and stabilize the shell suspension. Following CEPA addition, the suspension was allowed to stir for an additional 10 min before analysis and storage. The resulting suspension was stable for more than a month at room temperature as determined by DLS measurements.

TEM Analysis. Carbon-coated 300-mesh copper grids with a Formvar support (Ted Pella) were used for particle visualization using a transmission electron microscope. After the reaction was completed a 1−2 μL drop of shaken solution was placed in the center of the grid and allowed to dry. No further staining or preparation was used. A JEOL 100-SX microscope operating at 100 kV was used to obtain images on Kodak 4489 electron film. The film was developed in Kodak D-19 developer according to the manufacturer's directions.

DLS Analysis. Undiluted, vacuum degassed nanoparticle suspensions were filtered through a 0.45-μm CA filter to remove large dust. A Coulter N4 Plus submicron particle sizer with a He−Ne laser and a detector angle of 90° was used for particle size measurements. Each 4-min scan was averaged 7 times to obtain a standard deviation of the distribution mean size. Reported average particle diameters were obtained from unimodal analysis, considering only samples with polydispersity indices less than 0.2.

AFM Analysis. Atomic force microscope images were obtained using a Multimode IIIa NanoScope (Digital Instruments) operating in tapping mode with OTESPA probes (Digital Instruments) of 15-nm nominal diameter. The same grid used for visualization by TEM was used for topographic imaging by AFM. TEM grids were fixed to an AFM sample puck (Ted Pella) with no further preparation. The NanoScope v. 5.12r3 software bearing analysis tool was used to determine the average height of the particles.

Free Calcium and pH Measurements. To estimate the total reaction time necessary for all the calcium and phosphate to react, the concentration of free calcium was monitored as a function of time with a Sure-Flow calcium sensitive combination electrode (model 9720BN from Orion). The pH was measured using an AccuFET pH electrode (Accumet) using a three point calibration. Both calcium concentration and pH were recorded with an AR60 dual channel pH/ISE meter (Accumet).

Stability Analysis. Dynamic light scattering was utilized to characterize the particle size distribution and suspension stability in the presence of salt and protein. Suspensions of shells with NaCl ranging from 25 to 200 mM were made in 25-mM increments and the size was tested with DLS after each run. Bovine serum albumin was added to a shell suspension to make a 2.5 g/dL solution and distribution with DLS after each run. Samples were monitored every day for a week to note any change.

Results

TEM Results. Figure 1 shows a typical sample of CEPA-coated dispersed shells obtained using DOPA liposomes. The magnified inset was taken from different samples and demonstrates the difference in shell thickness obtained by adding CEPA at later (I) and earlier (II) times. When CEPA was added within 15 min of the initiation of the reaction, liposomes with thin shells of calcium phosphate were obtained, whereas noticeably thicker shells were obtained when CEPA was added 150 min after initiation (Figure 2).

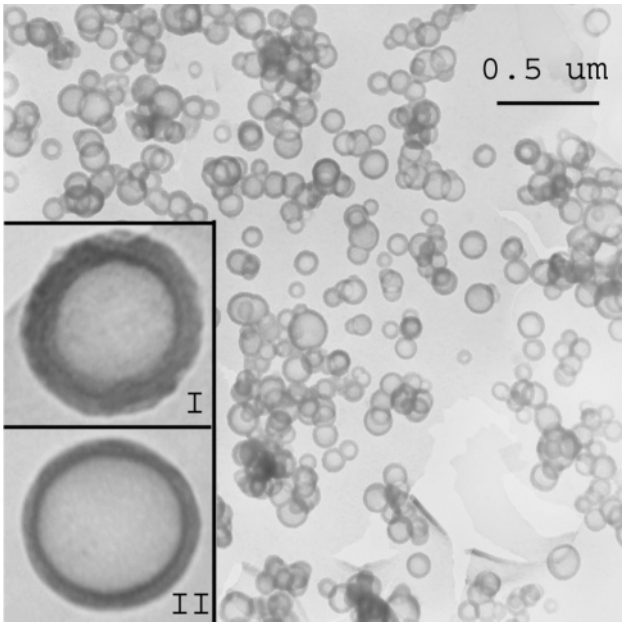

Figure 1. TEM image demonstrating morphology of calcium phosphate coated liposomes. Some clustering is typically seen on TEM grids as an artifact of the drying process. The inset shows the difference in shell thickness obtained when CEPA is added at different times.

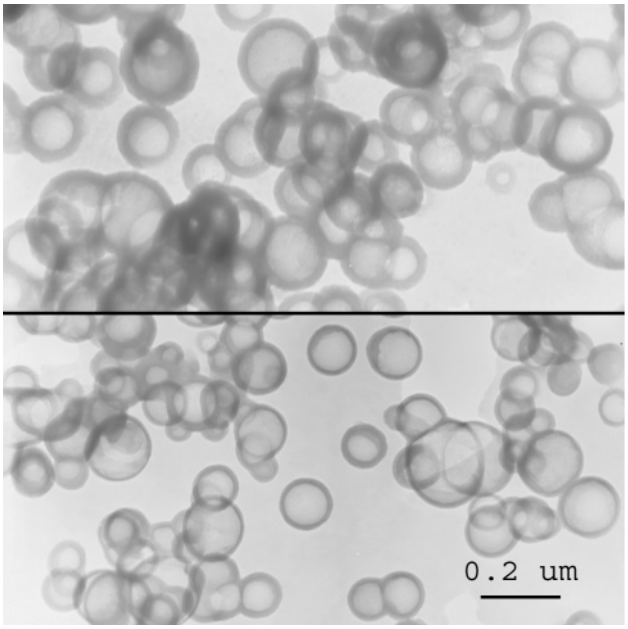

Figure 2. TEM image of thick- and thin-walled calcium phosphate coated liposomes obtained by addition of CEPA at 15 min (lower) and 150 min (upper) after the start of the reaction.

The dominant particle morphology in suspension was shells with the possibility of some small crystallites that form on the walls of the container or nucleate around atmospheric dust. During drying, shells could cluster together as shown in Figure 3 but the problem was less severe for CEPA-coated shells. Particles aged for several hours without addition of CEPA formed needle-shaped

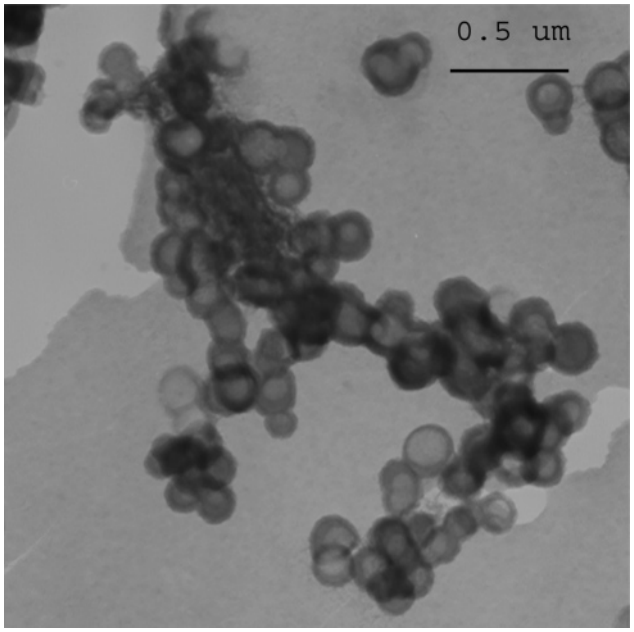

Figure 3. TEM image demonstrating the clustering of shells that can occur during drying of the suspension of the particles on the TEM grid or during certain synthesis conditions.

crystals on their exterior and also clustered upon drying. During drying of the TEM grid, water evaporation raises the concentration of free ions and their degree of saturation with respect to the solid phase. During this time all the ions from the originally equilibrated solution crystallize once there is insufficient water to support their hydration. Possible products of this process include heterogeneous nucleation onto small crystallites, the shells, atmospheric dust, or defects in the grid, or homogeneous nucleation of solid inorganic particles may occur. Crystallites of various shapes and sizes, some large dendritic growth, salt crystals, and shell clusters may be seen. To ensure that these micrometer-size aggregates are the result of drying and not present in solution, a filtered sample and a nonfiltered sample were analyzed by DLS. The maximum size of the particle distribution did not exceed 500 nm for 3 different samples with CEPA addition times of 15, 60, and 150 min with or without filtering through a 0.45-μm filter. Short dialysis ($\sim$1 h) against DI removed many of the free ions and reduced the appearance of these secondary structures.

DLS Results. Figure 4 shows the trend of mean particle sizes obtained from DLS for samples by addition of CEPA at varying delay times after the initiation of the reaction. Plotted is the average of 8 experiments for each delay time prior to CEPA addition. As the delay time was increased from 10 to 180 min the particle size increased from 120 to 180 nm. Figure 5 shows typical DLS unimodal size distribution curves obtained from the starting liposome suspension, and for the largest product obtained when CEPA was added 2.5 h after the initiation of the reaction. Samples analyzed without filtering revealed all particles were less than 400 nm.

AFM Results. Atomic force microscopy was used to confirm the spherical morphology of the particles as well as to confirm the particle sizes obtained from DLS. Figure 6 shows a 15 $\times$ 15 μm section of a TEM grid with dispersed spherical particles and some aggregates from

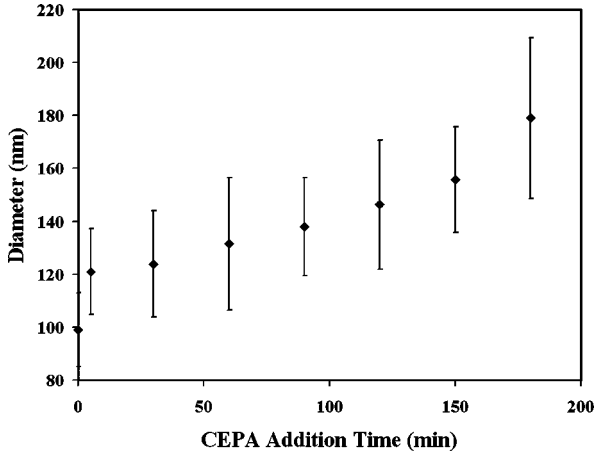

Figure 4. Dependence of particle size and hence shell thickness on the time at which the capping molecule CEPA is added. All particles use the same size liposome template.

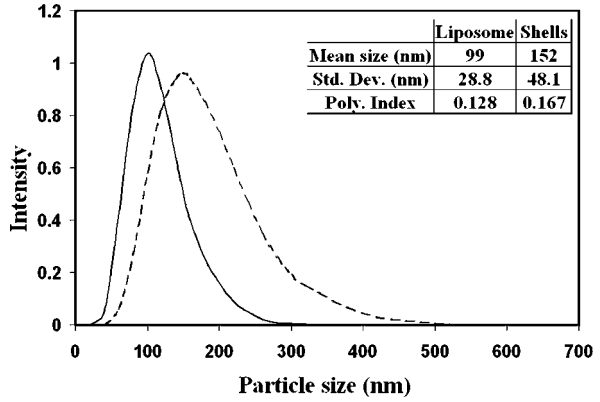

Figure 5. Typical DLS curves for liposome suspensions and shell suspensions. The broadening of the peak is due to the inherent uneven growth of the shells around the liposomes.

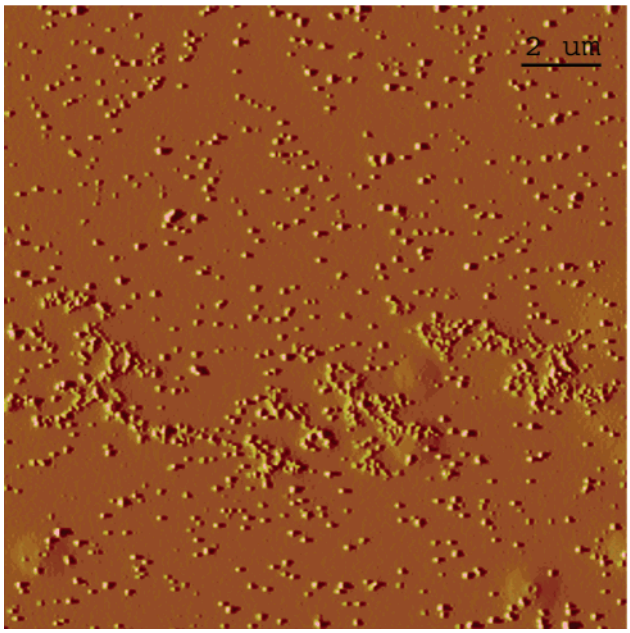

Figure 6. AFM image of shells on a TEM grid also seen in Figure 1. The size distribution from a bearing analysis is 117 nm which agrees well with DLS.

samples for which CEPA was added 15 min after initiation of the reaction. The pixel height histogram of this image showed a mean size of 117 nm and a

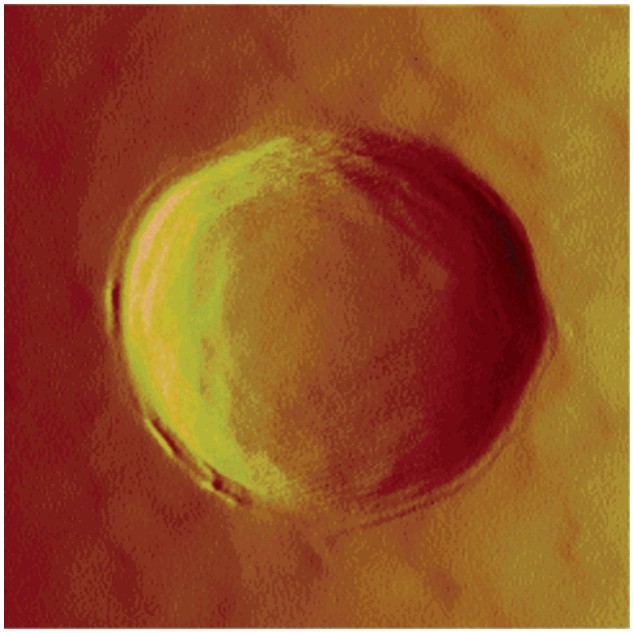

Figure 7. AFM image showing the uneven surface morphology of an individual calcium phosphate shell.

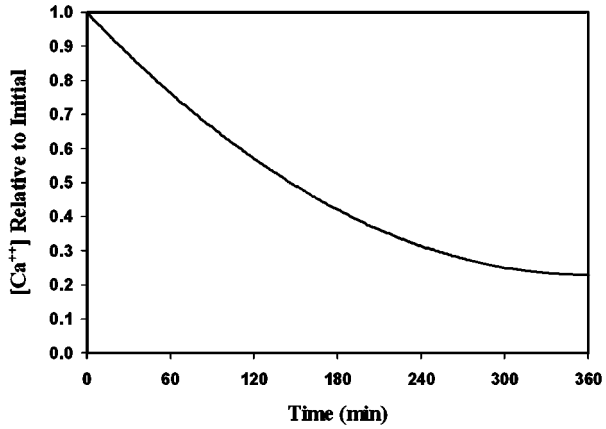

Figure 8. Relative calcium concentration versus time obtained from calcium probe data demonstrating the average length of the shell formation reaction. The line shown is a trend of the average signal over time.

standard deviation of ±16 nm and agrees well with the particle size obtained from DLS. Figure 7 shows a magnified AFM image of one of the particles.

Free Calcium Measurements. Once the reaction is initiated, it can be seen from the trend in Figure 8 that the normalized calcium concentration decreases gradually over the course of approximately 6 h, indicating the end of the reaction. During this period the CEPA can be added to obtain a specific mean shell thickness. It is possible to lengthen the total time of reaction by either reducing pH or reducing concentration of phosphates or calcium.

Measurement of Solution Stability. When the shells were introduced to a 0.2 M NaCl solution, the mean size did not vary by more than 7% of the initial value of 124 nm with and without filtering. When 2.5 g/dL of albumin was added to the shell suspension, the mean size of the suspension obtained by unimodal analysis decreased to 77 nm which occurs due to scattering contributions of the small protein molecules

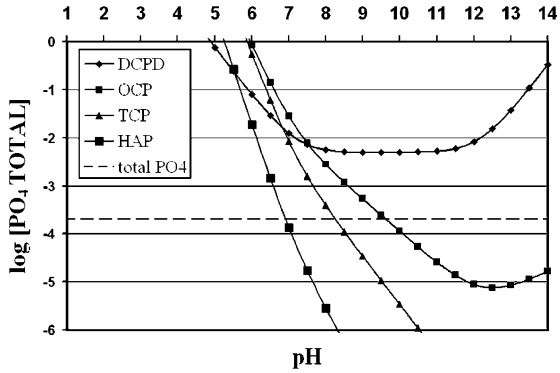

Figure 9. Calculated solubility isotherms for the different crystalline forms of calcium phosphate used in selecting initial reaction conditions.

which shifted the mean to a lower value. The measured mean sizes of either solution did not change over a week.

Discussion

In this work the synthesis of calcium phosphate nanoshells was demonstrated using a novel batch method in which DOPA liposomes were introduced into a supersaturated solution of calcium phosphate that then precipitated on the periphery of the liposomes. Our previous method[11] involved the slow titration of a liposome suspension with dilute concentrations of calcium and phosphate salts. That method was found to be inconvenient for scale-up and was sensitive to small changes in the concentration and addition rate of reagents. In this method the shell formation rate was controlled by pH and degree of solution supersaturation with respect to calcium phosphate. Particle growth could be stopped by adding a capping molecule to prevent the reaction and stabilize the particles.

DOPA was chosen as a lipid because it readily forms liposomes, has a T_c less than 45 °C rendering it amenable to hand extrusion, and has a negatively charged phosphatidic acid headgroup which aids in the localization of ions around the liposome. These three factors were found to be most important when selecting the lipid for this type of synthesis. Selected lipids must readily form stable liposomes at room temperatures because if the bilayer is unstable it is likely to deform or rupture as it complexes with precipitating ions. While it is possible that other interesting morphologies may arise they are not the main interest of this work and so were avoided through appropriate lipid selection. In order for the calcium phosphate to crystallize around the liposome, there must be a driving force for the reaction to occur. In this case it is the thermodynamic stability of the solid calcium phosphate phase in a supersaturated solution.

The solubility diagram in Figure 9 can be helpful in selecting successful synthesis conditions. Detailed information on calcium phosphate solubility and dissolution can be found elsewhere.[21–24] The calcium phosphate

(21) Brown, W. E.; Chow, L. C. *J. Cryst. Growth* **1980**, 31.
(22) van Kemenade, M. J. J. M.; de Bruyn, P. L. *J. Colloid Interface Sci.* **1987**, *2*, 564.
(23) Barone, J. P.; Nancollas, G. H. *J. Colloid Interface. Sci.* **1977**, *3*, 421.
(24) Christoffersen, J.; Christoffersen, M. R.; Kjaergaard, N. *J. Cryst. Growth* **1978**, *43*, 501.

system is more complicated than that of simple crystals such as NaCl because it can form more than one crystalline phase. In order of increasing stability, the five stoichiometrically distinct phases are amorphous calcium phosphate (ACP), dicalcium phosphate dihydrate [$CaHPO_4 \cdot 2H_2O$] (DCPD), octocalcium phosphate [$Ca_8(HPO_4)_2(PO_4)_4$] (OCP), tricalcium phosphate [$Ca_3(PO_4)_2$] (TCP), and hydroxyapatite [$Ca_{10}(PO_4)_6OH_2$] (HAP). The solubility of a particular calcium phosphate solid phase is dependent primarily on pH and the activity of the ions in solution. To obtain the solubility isotherm for the calcium phosphate system at 25 °C the conditions that satisfied $K_{sp} = IP$ were found where K_{sp} is the solubility product constant and IP is the ion product of the crystalline form. The IP is dependent on ion activities (f_i), which were determined using the Debye−Huckel equation. For a general calcium phosphate $Ca_vH_w(HPO_4)_x(PO_4)_yOH_z$ the ion product is of the following form:

$$IP = ([Ca^{2+}]f_{Ca})^v([H^+]f_H)^w([HPO_4{}^{2-}]f_{HPO4})^x \times ([PO_4{}^{3-}]f_{PO4})^y([OH^-]f_{OH})^z$$

The concentration of phosphate ions was obtained from the pK_a values of the phosphate system.

For crystallization to occur at a given pH, temperature, and salt concentration, the calcium phosphate concentration in solution must be supersaturated with respect to the solid phase. The lines plotted in Figure 9 are a guide to the thermodynamic stability of the system, but kinetic factors also influence what is produced. The Ostwald rule of stages[25] suggests the least stable form of a crystal forms first even though the degree of supersaturation or thermodynamic driving force is less than the more stable phases. It is thought these unstable clusters of ACP act as nucleation sites on which the more stable and often slower growing crystals form. In the case of calcium phosphate shell formation it is probable that initially an unstable coating of ACP forms and as time goes on this coating can act a nucleating site for the other more stable forms of calcium phosphate. The exact stoichiometry of the shell can vary and no crystalline peaks were observed using X-ray diffraction leaving the precise chemistry of the shell unknown.

It is hypothesized that the formation of calcium phosphate coating on the exterior of the liposomes is initiated by electrostatic localization of free ions around the liposome, thereby raising the local concentration much higher than in bulk solution. In the case of negatively charged DOPA liposomes the Ca^{2+} and Na^+ ions are electrostatically attracted by the negative exterior charge and form a Stern Layer on the liposomes while a diffuse layer of H_xPO_4 ($x = 0, 1, 2$) and Cl^- ions is formed around it. The formation of this electric double layer effectively increases the local concentration of the calcium and phosphate above the saturation point and causes crystallization to preferentially occur near the surface of the liposome. As time goes on, the inorganic phase continues to grow on the exterior until equilibrium between the solid and ions in solution is reached. To control the thickness of the shell, the solution must be tuned to reach equilibrium as the shell reaches the desired thickness. In practice, selection of initial conditions to achieve this desired outcome is difficult and it is necessary to monitor the concentration and rate of depletion of free ions during the reaction. Instead, an alternative method of controlling shell thickness was devised using CEPA as a capping molecule. CEPA was added at selected times during active shell growth based on total reaction times determined from free calcium measurements. After CEPA addition the solution was incubated for 30 min then the unreacted calcium and phosphate were dialyzed out. The product of this reaction was calcium phosphate shells encapsulating liposome lipid bilayers, and a spherical aqueous compartment, with a layer of exposed COO^- groups. An added benefit is the enhanced stability of the suspension in the presence of 0.2 mM salt in 2.5 g/dL albumin.

The initial concentration of reactants governs the kinetics of the reaction and final equilibrium condition. If the initial concentration is high then the reaction will proceed faster and the CEPA will need to be added at an earlier time to obtain shells of similar thickness and vice versa. Lower concentrations of calcium and phosphate have the dual advantage of a decrease in side reactions and a longer time window during which CEPA can be added, allowing finer control of the mean size. The phosphate ion concentration is pH dependent. As pH increases, the concentrations of the two reactive phosphate species, HPO_4^{2-} and PO_4^{3-}, are increased, affecting the reaction rate similarly to an increase in the concentration of phosphate.

Liposome concentration proportionately affects the nanoshell yield. If it becomes too high the liposome−liposome collision frequency is increased, and one of two things can happen. The bilayers of the liposomes could interact with each other forming an assortment of nonspherical, multilamellar, or larger liposomes. The shells may also form aggregates in solution held together by calcium phosphate linkages as they grow. The mechanism by which these aggregates form is different from that which causes clusters to form as the grid dries which is caused by surface energy minimization.

Finally, ionic strength changes across the lipid bilayer should be kept to a minimum so the membrane does not destabilize. If the ionic strength gradient across the membrane is too high the liposome will shrink in an effort to increase the interior ionic strength and smaller daughter vesicles will pinch off. Likewise, if it is too low the liposome ruptures and the free lipids form a random assortment of bilayer and micellar structures that eventually can be calcified. These well-known effects are described elsewhere.[26−29]

Aqueous-cored calcium phosphate nanoparticles may be suited for delivery of hydrophilic drug substances. The liposome-templated design can be more flexible than drug-coated powders,[30,31] or randomly coprecipi-

(25) Feenstra, T. P.; de Bruyn, P. L. *J. Colloid Interface Sci.* **1981**, *1*, 66.

(26) Menager, C.; Cabuil, V. *J. Phys. Chem. B*. **2002**, *32*, 7913.

(27) Bernard, A. L.; Guedeau-Boudeville, M. A.; Jullien, L.; di Meglio, J.-M. *Biochim. Biophys. Acta - Biomembranes* **2002**, *1−2*, 1.

(28) Milon, A.; Lazrak, T.; Albrecht, A. M.; Wolff, G.; Weill, g.; Ourisson, G.; Nakatani, Y. *Biochim. Biophys. Acta* **1986**, *1*, 1.

(29) Ghosh, P.; Singh, U. N. *Biochim. Biophys. Acta* **1992**, *1*, 88.

(30) Guicheux, J.; Grimandi, G.; Trecant, M.; Faivre, A.; Takahashi, S.; Daculsi, Guy *J. Biomed. Mater. Res*. **1997**, 34, 165.

tated materials[32] because their load capacity can be manipulated by the solubility of the encapsulant and the liposome size, without affecting the self-assembly of the organic coating. Variation of coating thickness and stoichiometry may be one means of manipulating the dissolution kinetics of the inorganic coating to control the release of encapsulated materials. Dissolution kinetics of these particles is likely to be determined by the coating thickness, stoichiometry of the mineral phase, pH, and the activity of phosphatases.

Conclusions

It is possible to form aqueous-cored calcium phosphate nanoparticles using liposome-templated self-assembly of calcium phosphate. The spherical morphology of the product was verified by AFM and the hollowness of the shell structure was verified using TEM. The mean size of these particles can be controlled by extrusion of the liposomes and the thickness of the organic coating can be controlled by adding the capping molecule CEPA at various times in the reaction. By varying the pH or concentration, the reaction time can be lengthened or shortened. The CEPA coating significantly improves their stability in salt and protein solutions.

Acknowledgment. H.T.S. thanks the Center for Molecularly Engineered Materials for financial support. Appreciation to Dr. Paul McGinn for use of Scintag XRD, Dr. Gregory Hartland for the use of the Coulter DLS machine, the Notre Dame Radiation Laboratory for use of their facilities and AFM, and Stephanie M. Schmidt for support and guidance.

CM040056I

(31) Trecant, M.; Guicheux, J.; Grimandi, G.; Leroy, M.; Daculsi, G. *Biomaterials* **1997**, 18, 141.
(32) Roy, I.; Mitra, S.; Maitra, A.; Mozumdar S. *Int. J. Pharm.* **2003**, 250, 25−33.